RSC Advances

PAPER

View Article Online
View Journal | View Issue

Cite this: *RSC Adv.*, 2017, **7**, 23970

New diterpene alkaloids from the marine sponge *Agelas mauritiana*†

Li-Li Hong,‡[a] Jia-Bao Sun,‡[a] Fan Yang,[a] Man Liu,[a] Jie Tang,[a] Fan Sun,[a] Wei-Hua Jiao,[a] Shu-Ping Wang,[a] Wei Zhang*[b] and Hou-Wen Lin *[a]

Received 1st March 2017
Accepted 21st April 2017

DOI: 10.1039/c7ra02547e

rsc.li/rsc-advances

Chemical investigation of an ethanol extract of the sponge *Agelas mauritiana* led to the isolation and characterization of five new diterpene alkaloids, namely, (−)-8′-oxo-agelasine B (**1**), (+)-agelasine B (**2**), (+)-8′-oxo-agelasine C (**3**), agelasine V (**4**), and (+)-8′-oxo-agelasine E (**5**), along with two known compounds, (−)-8′-oxo-agelasine D (**6**), and agelasine D (**7**). The structures of these compounds were determined by interpretation of spectroscopic data and comparison with literature properties. Compounds **1** and **3–5** are the second example of 8′-oxo-agelasine analogs. Compounds **2** and **7** not only exhibited moderate cytotoxicity toward the cancer cell lines PC9, A549, HepG2, MCF-7, and U937 with IC_{50} values of 4.49–14.41 μM, but also showed potent antibacterial activities against a panel of methicillin-resistant *Staphylococcus aureus* (MRSA) clinical isolates with MIC_{90} values of 1–8 μg mL^{-1}.

Introduction

Marine sponges are distinguished as excellent sources for marine natural products, with 283 new compounds reported in 2014 alone.[1,2] The *Agelas* genus is a prolific producer of secondary metabolites containing bromopyrrole derivatives,[3,4] sesqui- and diterpenoid alkaloids,[5] glycosphingolipids,[6] carotenoids,[7] steroids,[8] and fatty acids.[9] Particularly, terpenoid alkaloids from this genus are attractive compounds, which are characterized by a sesqui- or diterpene unit attached to different polar functional groups including 6-amino-5-(formylamino)-4-(methylamino)-1,3-diazine, guanidine, sulfone, and methyladeninum. Since the first sesquiterpenoid alkaloid, agelasidine A, was isolated from the Sponge *Agelas* sp. in 1983, an array of terpenoid alkaloids have been reported to date.[10] These terpenoid derivatives are listed as agelasidines,[10–15] agelines,[16] agelasines,[5,15,17–24] agelasimines,[25] gelasines,[18] and axistatins,[26] which show interesting biological effects, such as cytotoxic,[14,18,25,26] anti-malarial,[23] anti-microbial,[11–14,16,22,24,26] antifouling,[19] antifungal,[15] as well as inhibitory effects on Na^+/K^+-ATPase.[11,17,20]

Our previous chemical investigation of the sponge *Agelas mauritiana* led to the isolation of four new antimicrobial alkaloids, in which (−)-8′-oxo-agelasine D was the first and the only 8′-oxo-agelasine reported to date.[12] As our continued exploration of this sponge in a search for structurally new products with promising bioactivities, we found that the CH_2Cl_2-soluble portion of an EtOH extract of the title sponge collected in March 2013, was cytotoxic against PC9, A549, and U937 cell lines in a Cell Counting Kit-8 (CCK-8) bioassay (8.5–10.5 μg mL^{-1}) and showed moderate antibacterial activity against methicillin-resistant *Staphylococcus aureus* (MRSA 2010-210) with MIC_{90} value of 1.0 μg mL^{-1}. Further bioactivity-guided fractionation of this CH_2Cl_2-soluble portion led to the isolation of five new compounds (**1–5**), as well as two known compounds (**6** and **7**). Compounds **1** and **3–5** represent the second example of 8′-oxo-agelasine analogs. All isolated compounds (**1–7**) were evaluated for their cytotoxic and antibacterial activities. Herein, we describe the isolation, structure elucidation, and bioactivities of **1–7**.

Results and discussion

Compound **1** was isolated as a pale yellow amorphous powder, and its molecular formula was deduced to be $C_{26}H_{39}N_5O$ from the HRESIMS ion at *m*/*z* 438.3232 $[M + H]^+$. The IR bands at 3325, 1718 cm^{-1} implied the presence of amino and carbonyl functionalities, respectively. UV absorption at 275 nm was in agreement with literature value[23] for purine moiety. The ^1H NMR spectrum of **1** displayed one deshielded aromatic siglet (δ_H 8.17), two exchangeable siglets (δ_H 7.36), one olefin siglet (δ_H 5.13), one olefin triplet (δ_H 5.28), four methyl siglets (δ_H 1.79, 0.95, 0.68, and 3.46), and two methyl doublets (δ_H 0.75 and 1.53). The ^{13}C NMR and HSQC spectra of **1** revealed 26 carbon signals corresponding to six methyls (including one nitrogen-bearing carbon at δ_C 26.8), seven methylenes, five methines, and eight quaternary carbons (including one carbonyl carbon at

[a]*Research Center for Marine Drugs, State Key Laboratory of Oncogenes and Related Genes, Department of Pharmacy, Renji Hospital, School of Medicine, Shanghai Jiao Tong University, Shanghai 200127, P. R. China. E-mail: franklin67@126.com*

[b]*Centre for Marine Bioproducts Development, Flinders University, Adelaide, SA 5042, Australia. E-mail: wei.zhang@flinders.edu.au*

† Electronic supplementary information (ESI) available: HRESIMS, 1D NMR, 2D NMR, IR, UV, and CD spectra. See DOI: 10.1039/c7ra02547e

‡ These authors contributed equally to this work.

δ_C 152.6). The above-mentioned NMR data exhibited close resemblance to those of agelasine B,[17] except for the purine unit. The corresponding sp^2 carbon in purine moiety at δ_C 141.7 in agelasine B[17] was replaced by a carbonyl carbon at δ_C 152.6 in **1**, which was established by the HMBC cross-peaks of the nitrogen methyl protons (δ_H 3.46) and C-4′ (δ_C 148.3) and C-8′ (δ_C 152.6), and of the aromatic proton (δ_H 8.17) and C-2′ (δ_C 146.3), C-4′ (δ_C 148.3), and C-5′ (δ_C 105.4) (Fig. 2). Moreover, a ^1H–^{15}N HMBC experiment was conducted to confirm this 8-oxo-9-*N*-methyladenine moiety. The observed ^1H–^{13}N HMBC correlations of H–NCH_3/N-9′ (δ_N 127.8), H_2-15 (δ_H 4.63)/N-7′ (δ_N 118.2), H-2′ (δ_H 8.17)/N-1′ (δ_N 193.3), and N-3′(δ_N 224.3) further prove this point. The rest $C_{20}H_{33}$ alkyl skeleton was assigned to have a clerodane skeleton by analysis of 2D NMR data (Fig. 2). In addition, HMBC correlations from two methylene protons (δ_H 4.63) to C-13 (δ_C 144.0), C-5′ (δ_C 105.4), and C-8′ (δ_C 152.6) suggested that the 9 *N*-methyladenine was attached to C-15 *via* N-7′.

The relative configuration of **1** was deduced from NOESY spectroscopic data (Fig. 3). The NOESY correlations of H_2-15 (δ_H 4.63)/H_3-16 (δ_H 1.79) and the chemical shift of C-16 (δ_C 16.9) indicated the 13*E*-configuration of the double bond Δ.[13,14] Cross-peaks of H_3-19 (δ_H 0.95)/H_3-20 (δ_H 0.68) and H-6a (δ_H 1.66), H_3-17 (δ_H 0.75)/H_3-20, H-10 (δ_H 1.27)/H-11a (δ_H 1.48), H-12b (δ_H 1.84), and H-6b (δ_H 1.12), and H-6b/H-8 (δ_H 1.40) indicated that H_3-17, H_3-19, H-6a, and H_3-20 were α-oriented while H-8, H-6b, H-10, and H_2-11 were β-oriented. Further comparison of the $[\alpha]_D^{25}$ values of **1** (−33.9, MeOH) with that of agelasine B (−21.5, MeOH[17] and −27.2 [27]) suggested the absolute configuration of **1** was probably identical to agelasine B since they had the same relative stereochemistry and the same sign of specific rotation. Thus, the structure of (−)-8′-oxo-agelasine B was concluded to be shown in Fig. 1.

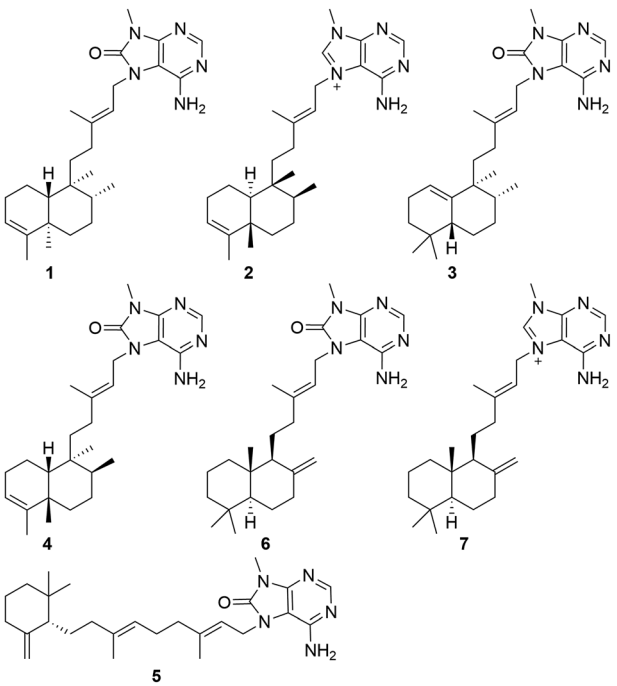

Fig. 1 The structures of compounds **1**–**7** from *Agelas mauritiana*.

Compound **2**, a white amorphous powder, possessed a molecular formula of $C_{26}H_{39}N_5$, according to its ^{13}C NMR and HRESIMS (*m*/*z* 422.3280 $[M + H]^+$, calcd for $C_{26}H_{40}N_5$, 422.3284) data. Detailed analysis of the 1D and 2D NMR spectral data revealed that the planar structure of **2** was the same as agelasine B (Fig. 2).[17] The double bond between C-13 (δ_C 146.2) and C-14 (δ_C 114.9) possessed the *E*-geometry, which was established by the NOESY correlations of H_2-15 (δ_H 5.16)/H_3-16 (δ_H 1.79) and H-14 (δ_H 5.45)/H_2-12 (δ_H 1.97, δ_H 1.87) and the chemical shift of C-16 (δ_C 16.7). Moreover, the α-configurations of H-6b (δ_H 1.10) and H-10 (δ_H 1.29) were derived from NOESY correlations for H-6b/H-10, while the β-configurations of H-6a (δ_H 1.65), H_3-17 (δ_H 0.78), H_3-19 (δ_H 0.95), and H_3-20 (δ_H 0.70) were implied from NOESY cross-peaks of H_3-19/H-6a and H_3-20 and H_3-17/H_3-20 (Fig. 4). The aforementioned data suggested **2** have identical

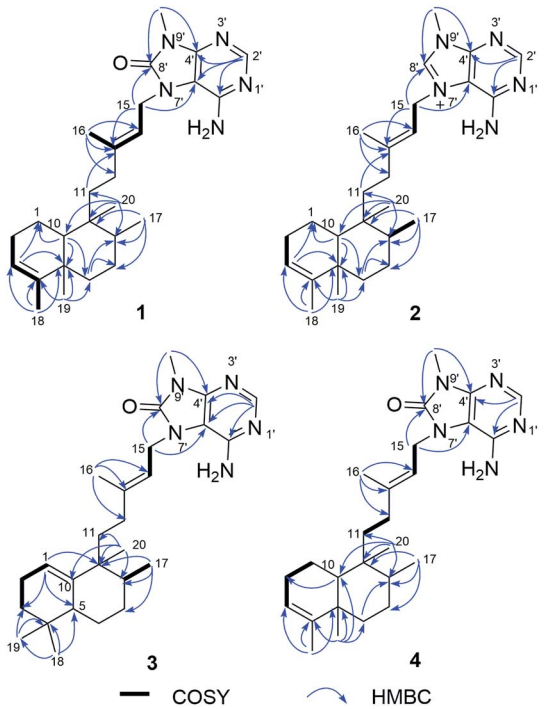

Fig. 2 Key ^1H–^1H COSY and HMBC correlations of compounds **1**–**4**.

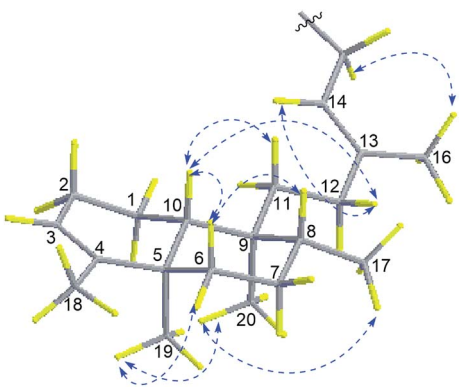

Fig. 3 Key NOESY correlations of compound **1**.

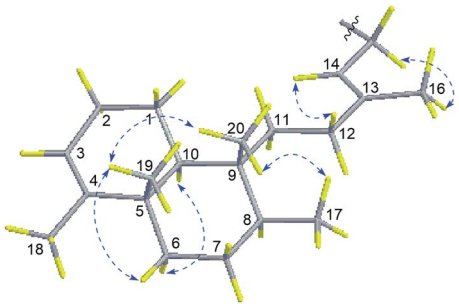

Fig. 4 Key NOESY correlations of compound **2**.

relative configuration with agelasine B. However, the opposite optical rotation data for them [**2** ($[\alpha]_D^{30}$ +22.7, MeOH), agelasine B ($[\alpha]_D^{25}$ −21.5, MeOH[17] and $[\alpha]_D^{25}$ −27.2 [27])] suggest **2** differed in absolute configuration at chiral centers with agelasine B. Thus, the structure of **2** was established as a stereoisomer of agelasine B and named (+)-agelasine B.

Compound **3** showed a $[M + H]^+$ ion peak at *m*/*z* 438.3231 in the HRESIMS, corresponding to a molecular formula of $C_{26}H_{39}N_5O$. Comparison of the ^1H and ^{13}C NMR spectroscopic data (Tables 1 and 2) of compound **2** suggested a rearranged labdane skeleton for **3**, which was further supported by the HMBC correlations from H_3-17 (δ_H 0.83) to C-7 (δ_C 31.2), C-8 (δ_C 44.5), and C-9 (δ_C 42.5), from H_3-20 (δ_H 1.00) to C-8, C-9, C-10 (δ_C 145.4), and C-11 (δ_C 29.6), from H_3-18 (δ_H 0.84) to C-3 (δ_C 31.3), C-4 (δ_C 31.2), C-5 (δ_C 43.8), and C-19 (δ_C 27.8), from H_3-19 (δ_H 0.84) to C-3, C-4, C-5, and C-18 (δ_C 27.8), from H-1 (δ_H 5.34) to C-3, C-5, and C-9, and from H-5 (δ_H 1.49) to C-1 (δ_C 117.6), C-3, C-7, C-10 (δ_C 145.4), C-18, and C-19 (Fig. 2). The 13*E*-configuration of the double bond $\Delta^{13,14}$ was inferred from the NOESY correlations of H_2-15 (δ_H 4.65)/H_3-16 (δ_H 1.79) and H-14 (δ_H 5.27)/H_2-12 (δ_H 1.81, δ_H 1.72) and the chemical shift of C-16 (δ_C 17.0). The NOESY correlations of H_3-17/H_3-20 and H-6a (δ_H 1.78) indicated the β-orientation of H_3-17, H-6a, and H_3-20, while the cross-peaks of H-5/H-6b (δ_H 1.73) and H-8 (δ_H 1.28)suggested these protons are α-oriented, establishing the relative configurations of **3** (Fig. 5), in consonance with those of the synthesis product (+)-agelasine C.[28] The absolute configurations of **3** was determined by comparison of its optical rotation $[\alpha]_D^{25}$ +29 (MeOH) and the synthesis product (+)-agelasine C $[\alpha]_D^{22}$ +25 (MeOH). Therefore, the structure of (+)-8′-oxo-agelasine C (**3**) was defined as shown in Fig. 1.

Compound **4** had a molecular formula of $C_{26}H_{39}N_5O$ based on the $[M + H]^+$ ion at *m*/*z* 438.3230 (calcd for $C_{26}H_{40}N_5O$, 438.3233) in the HRESIMS. Extensive analysis of HMBC and COSY correlations revealed that compound **4** shared the same planar structure as **1** (Fig. 2). The NOESY correlation of H_2-15

Table 1 ^1H NMR spectroscopic data for compounds **1**–**5** (δ in ppm, *J* in Hz)

Position	**1**[a,c]	**2**[a,d]	**3**[a,c]	**4**[b,c]	**5**[b,c]
1a	1.38, m	1.54, m	5.34, m	1.83, m	2.00, m
1b				1.59, m	
2a	1.99, m	1.98, m	2.01, m	1.97, m	1.53, m
2b	1.92, m				
3a	5.13, s	5.13, s	1.38, m	5.34, m	1.46, m
3b			1.06, m		1.21, m
5			1.49, dd (12.6, 3.0)		1.67, m
6a	1.66, d (12.6)	1.65, dt (13.2, 3.0)	1.78, m	1.62, m	1.38, m
6b	1.12, m	1.10, m	1.73, m	1.48, m	
7a	1.92, m	1.46, m	1.41, dd (13.2, 3.6)	1.43, m	1.74, m
7b	1.37, m	1.38, m	1.09, m	1.34, m	
8	1.40, m	1.42, m	1.28, m	1.55, m	
9					5.03, s
10	1.27, m	1.29, d (12.6)		1.41, m	
11a	1.48, m	1.47, m	1.25, s	1.83, m	2.11, m
11b	1.29, m	1.35, m		1.24, m	
12a	1.92, m	1.97, m	1.81, m	2.12, td (13.2, 4.0)	2.11, m
12b	1.84, td (12.6, 4.8)	1.87, td (12.6, 4.8)	1.72, m	2.00, m	
14	5.28, t (6.0)	5.45, t (6.0)	5.27, t (6.0)	5.35, m	5.34, t (5.6)
15	4.63, d (6.0)	5.16, d (6.0)	4.65, d (6.0)	4.68, d (5.6)	4.67, d (5.6)
16	1.79, s	1.79, s	1.79, d (1.2)	1.83, s	1.82, s
17	0.75, d (5.4)	0.78, d (6.6)	0.83, s	0.85, d (7.2)	1.58, s
18	1.53, d (1.8)	1.54, d (1.2)	0.84, s	1.62, s	0.90, s
19	0.95, s	0.95, s	0.84, s	1.12, s	0.82, s
20a	0.68, s	0.70, s	1.00, s	1.01, s	4.74, s
20b					4.52, d (2.0)
2′	8.17, s	8.46, s	8.18, s	8.19	8.18, s
8′		9.54, s			
2′-NH_2	7.36, br s	7.90, br s	7.62, br s	7.69, br s	7.66, br s
9′-CH_3	3.46, s	3.89, s	3.50, s	3.51, s	3.50, s

[a] Measured at 600 MHz. [b] Measured at 400 MHz. [c] Measured in $CDCl_3$. [d] Measured in DMSO-d_6.

Table 2 ^{13}C NMR spectroscopic data for compounds **1**–**5** (δ in ppm)

Position	**1**[a,c]	**2**[a,d]	**3**[a,c]	**4**[b,c]	**5**[b,c]
1	18.3, CH_2	17.8, CH_2	117.6, CH	19.9, CH_2	32.5, CH_2
2	26.8, CH_2	26.3, CH_2	23.2, CH_2	25.7, CH_2	23.7, CH_2
3	120.3, CH	120.2, CH	31.3, CH_2	122.5, CH	36.3, CH_2
4	144.3, C	143.6, C	31.2, C	141.8, C	34.9, C
5	38.1, C	37.6, C	43.8, CH	38.7, C	53.6, CH
6	36.7, CH_2	36.2, CH_2	30.1, CH_2	32.1, CH_2	24.8, CH_2
7	27.4, CH_2	27.0, CH_2	31.2, CH_2	27.2, CH_2	38.2, CH_2
8	36.2, CH	35.7, CH	44.5, CH	37.4, CH	137.0, C
9	38.6, C	38.2, C	42.5, C	38.7, C	122.5, CH
10	46.4, CH	45.9, CH	145.4, C	44.6, CH	149.3, C
11	36.4, CH_2	35.8, CH_2	29.6, CH_2	36.0, CH_2	26.1, CH_2
12	33.0, CH_2	32.5, CH_2	33.9, CH_2	33.7, CH_2	39.5, CH_2
13	144.0, C	146.2, C	144.7, C	144.7, C	143.3, C
14	119.5, CH	114.9, CH	119.3, CH	119.5, CH	119.8, CH
15	40.5, CH_2	47.0, CH_2	40.6, CH_2	40.6, CH_2	40.6, CH_2
16	16.9, CH_3	16.7, CH_3	17.0, CH_3	17.1, CH_3	16.9, CH_3
17	15.9, CH_3	15.8, CH_3	16.3, CH_3	15.3, CH_3	16.1, CH_3
18	17.9, CH_3	17.7, CH_3	27.8, CH_3	19.3, CH_3	28.4, CH_3
19	19.8, CH_3	19.6, CH_3	27.8, CH_3	28.0, CH_3	26.2, CH_3
20	18.2, CH_3	18.1, CH_3	23.0, CH_3	26.2, CH_3	108.8, CH_2
2′	146.3, CH	155.4, CH	145.8, CH	145.6, CH	145.6, CH
4′	148.3, C	148.9, C	148.3, C	148.3, C	148.3, C
5′	105.4, C	109.2, C	105.4, C	105.4, C	105.4, C
6′	143.6, C	152.3, C	143.5, C	143.4, C	143.3, C
8′	152.6, C	140.9, CH	152.6, C	152.6, C	152.6, C
9′-CH_3	26.8, CH_3	31.4, CH_3	26.9, CH_3	26.9, CH_3	26.9, CH_3

[a] Measured at 150 MHz. [b] Measured at 100 MHz. [c] Measured in $CDCl_3$. [d] Measured in DMSO-d_6.

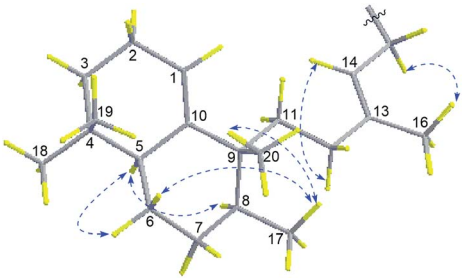

Fig. 5 Key NOESY correlations of compound **3**.

(δ_H 4.68)/H_3-16 (δ_H 1.83) and H-14 (δ_H 5.35)/H_2-12 (δ_H 2.12 and 2.00) and the chemical shift of C-16 (δ_C 17.1) suggested the *E*-geometry of the $\Delta^{13,14}$ double bond. The NOESY cross-peaks of H_3-17 (δ_H 0.85)/H-11b (δ_H 1.24) and H-10 (δ_H 1.41), H-10/H-12a (δ_H 2.12), H_2-11 (δ_H 1.83 and 1.24), H_3-19 (δ_H 1.12) and H-6a (δ_H 1.62), and H_3-19/H-6a located H_3-17, H-10, H-6a, and H_3-19 on the same face, while NOESY correlation of H_3-20 (δ_H 1.01)/H-8 (δ_H 1.55) positioned H_3-20 and H-8 on the opposite face (Fig. 6). Thus, the structure of **4** was assigned as a stereoisomer of agelasine B and named agelasine V.

Compound **5**, a pale yellow amorphous powder, had a molecular formula of $C_{26}H_{39}N_5O$ deduced from the ^{13}C NMR and HRESIMS (438.3229 $[M + H]^+$, calcd for $C_{26}H_{40}N_5O$, 438.3233) data. Compound **5** possessed the same 8-oxo-9-*N*-methyladenine moiety according to the comparison of its 1D

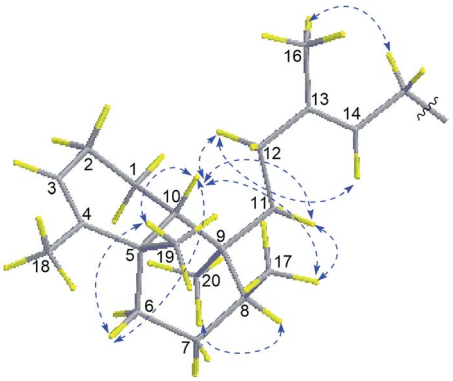

Fig. 6 Key NOESY correlations of compound **4**.

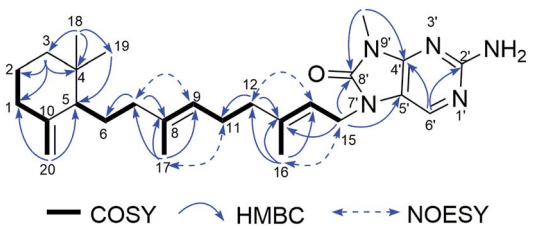

Fig. 7 Key ^{1}H–^{1}H COSY, HMBC and NOESY correlations of compound **5**.

NMR data (Tables 1 and 2) with those of compound **1**. The rest 9, 10-seco-labdane skeleton was determined by analysis of 2D NMR data (Fig. 7). The configurations of the double bonds ($\Delta^{9,10}$ and $\Delta^{13,14}$) were established as *E* based on the NOESY correlations of H_3-17 (δ_H 1.58)/H_2-11 (δ_H 2.11), H-9 (δ_H 5.03)/H_2-7 (δ_H 1.74), H_3-16 (δ_H 1.82)/H_2-15 (δ_H 4.67), and H_2-12 (δ_H 2.11)/H-14 (δ_H 5.34) and the chemical shift of C-17 (δ_C 16.1) and C-16 (δ_C 16.9). The absolute configuration of **5** was assumed to be the same as (+)-trixagol, whose enantiomer was equate to the terpenoid side chain of (−)-agelasine E in that they both exhibit positive optical rotations [**5** ($[\alpha]_D^{30}$ +30.6, MeOH), (+)-trixagol ($[\alpha]_D$+14, $CHCl_3$)[29] and agelasine E ($[\alpha]_D^{25}$ −17.1, MeOH)[20]]. Accordingly, The structure of (+)-8′-oxo-agelasine E (**5**) was proposed as shown Fig. 1.

All isolated compounds were assessed for their antibacterial activity against a methicillin-susceptible *S. aureus* (MSSA) strain H608 and four methicillin-resistant *S. aureus* (MRSA) strains 2010-260, 2010-210, 2010-292, and 2010-300. As shown in Table 3, compounds **2** and **7** exhibited potent activities against MRSA with MIC_{90} values of 1–8 μg mL^{-1} while other compounds showed no activity (MIC_{90} > 64 μg mL^{-1}). The cytotoxic activities of individual compounds were evaluated against the PC9, A549, HepG2, MCF-7, and U937 cell lines using Cell Counting Kit-8 (CCK-8) bioassay (Table 3). Compounds **2** and **7** showed moderate activities against the five cancer cell lines with IC_{50} values of 4.49–14.41 μM. Other compounds showed no activity (IC_{50} > 20 μM) except compound **6** show weak cytotoxicity against U937 cell line with IC_{50} value of 16.89 μM.

Table 3 Antibacterial and cytotoxic activities of compounds 1–7

Compounds[a]	Antibacterial activity against clinical MRSA[d] and MSSA[e] strains (MIC_{90}, μg mL^{-1})					Cytotoxic activity (IC_{50}, μM)				
	2010-260	2010-210	2010-292	2010-300	H608	PC9	A549	HepG2	MCF-7	U937
2	2	1	2	1	2	5.08	14.07	9.76	7.64	4.49
6	>64	>64	>64	>64	>64	>50	>50	>50	>50	16.89
7	4	4	8	8	1	4.49	14.41	10.07	5.47	6.86
Vancomycin[b]	1	1	1	0.5	2					
Doxorubicin[c]						0.22	0.49	0.20	0.38	0.05

[a] Compounds **1** and **3–5** were inactive in all assays. [b] Positive control for antibacterial assay. [c] Positive control for cytotoxic assay. [d] Clinical MRSA strains 2010-260, 2010-210, 2010-292, 2010-300. [e] Clinical MSSA strain H608.

Conclusions

In conclusion, five new diterpene alkaloids, illustrated by (−)-8′-oxo-agelasine B (**1**), (+)-agelasine B (**2**), (+)-8′-oxo-agelasine C (**3**), agelasine V (**4**), (+)-8′-oxo-agelasine E (**5**), along with two known related metabolites, (−)-8′-oxo-agelasine D (**6**), agelasine D (**7**), were isolated from the marine sponge *Agelas mauritiana*. The structures of them were established by interpretation of spectroscopic data and comparison with literature properties. Isolation of compounds **1** and **3–5** provided new examples of 8′-oxo-agelasine analogs. Compounds **2** and **7** showed potent antibacterial and moderate cytotoxic activities. Analysis of the structures of the diterpene alkaloids (**1–7**) and their antibacterial and cytotoxic activities led to a preliminary summary of the structure–activity relationship (SAR): C-8′-carbonylated compounds (**1** and **3–6**) can provide lower antibacterial and cytotoxic activities than other analogs (**2** and **7**). Moreover, the interesting antibacterial activity of compounds **2** and **7** indicated that they could be possible lead candidates as promising anti-MRSA agents.

Experimental section

General experimental procedures

Optical rotation data were measured in MeOH on an Autopol I polarimeter (no. 30575, Rudolph Research Analytical) with a 10 cm length cell. UV were recorded on a Hitachi U-3010 spectrophotometer. IR (KBr) spectra were obtained on Jasco FTIR-400 spectrometer. 1D and 2D NMR spectra were recorded in DMSO-d_6 or $CDCl_3$ on a Bruker DRX-600 or on a Bruker DRX-400 MHz NMR spectrometers. HRESIMS data was recorded on a Q-TOF micro YA019 mass spectrometer. Column chromatography (CC) was carried out on Sephadex LH-20 (Amersham Pharmacia Biotech AB), silica gel (200-300 mesh, Qingdao Marine Chemical Inc. China), and reverse phase C18 silica gel (15 μm, Santai Technologies, Inc.). Analytical thin-layer chromatography was carried out using HSGF 254 plates and visualized by spraying with anisaldehyde-H_2SO_4 reagent. Reversed-phase high-performance liquid chromatography (HPLC) was performed on Waters SunFire™ Prep C18 column (5 μm, 19 × 150 mm) with a Waters 1525 separation module equipped with a Waters 2998 photodiode array detector, and all solvents used for HPLC were of HPLC grade.

Animal material

Samples of *Agelas mauritiana* were collected along the coast of Yongxing Island in the South China Sea on March 19, 2013. A voucher specimen (no. 13-7) has been deposited at Research Center for Marine Drugs, State Key Laboratory of Oncogenes and Related Genes, Shanghai Jiao Tong University.

Extraction and isolation

The sponge (1.2 kg, wet weight) was cut and percolated with 95% EtOH at room temperature to afford the crude extract (15.2 g), which was suspended in H_2O and extracted with EtOAc. The EtOAc-soluble extract (9.3 g) was concentrated under reduced pressure. Subsequently, the EtOAc-soluble extract was partitioned between 90% aqueous MeOH and petroleum ether to give 5.5 g petroleum ether-soluble fraction. The 90% aqueous MeOH fraction was diluted to 60% aqueous MeOH with H_2O and extracted with CH_2Cl_2 to afford a 4.5 g CH_2Cl_2-soluble fraction. This CH_2Cl_2-soluble extract was chromatographed on silica gel column eluting with a step gradient of CH_2Cl_2–MeOH (100 : 1 to 0 : 1) to give nine fractions (DA–DI). Fraction DH (1.1 g) was subjected to VLC over silica gel eluting with a CH_2Cl_2–EtOAc–MeOH–H_2O system (10 : 5 : 1.5 : 0.2 and 0 : 0 : 1 : 0) to afford four subfractions (DH1–DH4). Subfraction DH3 (200.1 mg) was directly separated by reversed-phase HPLC (Waters SunFire™ Prep C18, 5 μm, 19 × 150 mm; 10.0 mL min^{-1}; 210, 270 nm) eluting with a CH_3CN–H_2O–TFA system (50 : 50 : 0.1) to give (+)-agelasine B (**2**, 40.0 mg, t_R 8.5 min) and agelasine D (**7**, 35.2 mg, t_R 10.0 min). DH1 (163.6 mg) was subjected to silica gel column chromatography, using a gradient of CH_2Cl_2–EtOAc–MeOH–H_2O solvent system (50 : 5:1 : 0.1, 45 : 5:1 : 0.1, 40 : 5:1 : 0.1, 25 : 5:1 : 0.1, 20 : 5:1 : 0.1, 20 : 5:1 : 0.1, 10 : 5:1.25 : 0.2, and 0 : 0:1 : 0) to give 5 subfractions (DH1A–DH1E). Subfraction DH1B (60.5 mg) was further purified by reversed-phase HPLC (Waters SunFire™ Prep C18, 5 μm, 19 × 150 mm; 9.0 mL min^{-1}; 210, 270 nm) eluting with a CH_3CN–H_2O–TFA (55 : 45 : 0.1) system to give (−)-8′-oxo-agelasine B (**1**, 15.0 mg, t_R 49.5 min), (−)-8′-oxo-agelasine D (**6**, 13.1 mg, t_R 55.0 min), (+)-8′-oxo-agelasine C (**3**, 5.7 mg, t_R 63.9 min), agelasine V (**4**, 2.8 mg, t_R 52.0 min), (+)-8′-oxo-agelasine E (**5**, 2.9 mg, t_R 70.0 min).

(−)-8′-Oxo-agelasine B (1). Pale yellow amorphous powder; $[\alpha]_D^{25}$ −33.9 (*c* 0.11, MeOH); UV (MeOH) λ_{max} (log ε) 216 (4.07),

275 (3.64) nm; IR (KBr) ν_{max} 3325, 2927, 2861, 1718, 1639, 1460, 1376, 1198, 1141 cm^{-1}; ^1H and ^{13}C NMR data, see Tables 1 and 2; HRESIMS *m/z* 438.3232 $[M + H]^+$ (calcd for $C_{26}H_{40}N_5O$, 438.3233).

(+)-Agelasine B (2). Pale yellow amorphous powder; $[\alpha]_D^{30}$ +22.7 (*c* 0.10, MeOH); UV (MeOH) λ_{max} (log ε) 214 (4.16), 262 (3.63) nm; IR (KBr) ν_{max} 3320, 2927, 2858, 1683, 1649, 1460, 1379, 1202, 1133, 798, 720 cm^{-1}; ^1H and ^{13}C NMR data, see Tables 1 and 2; HRESIMS *m/z* 422.3280 $[M + H]^+$ (calcd for $C_{26}H_{40}N_5$, 422.3284).

(+)-8′-Oxo-agelasine C (3). Pale yellow amorphous powder; $[\alpha]_D^{25}$ +29.0 (*c* 0.08, MeOH); UV (MeOH) λ_{max} (log ε) 214 (4.00), 274 (3.50) nm; IR (KBr) ν_{max} 3325, 2925, 2856, 1721, 1640, 1459, 1373, 1197, 1142 cm^{-1}; ^1H and ^{13}C NMR data, see Tables 1 and 2; HRESIMS *m/z* 438.3231 $[M + H]^+$ (calcd for $C_{26}H_{40}N_5O$, 438.3233).

Agelasine V (4). Pale yellow amorphous powder; $[\alpha]_D^{30}$ +36.5 (*c* 0.08, MeOH); UV (MeOH) λ_{max} (log ε) 214 (3.62), 275 (3.12) nm; IR (KBr) ν_{max} 3330, 2926, 2856, 1721, 1641, 1461, 1375, 1198, 1092, 802 cm^{-1}; ^1H and ^{13}C NMR data, see Tables 1 and 2; HRESIMS *m/z* 438.3230 $[M + H]^+$ (calcd for $C_{26}H_{40}N_5O$, 438.3233).

(+)-8′-Oxo-agelasine E (5). Pale yellow amorphous powder; $[\alpha]_D^{30}$ +30.6 (*c* 0.11, MeOH); UV (MeOH) λ_{max} (log ε) 203 (3.58), 275 (3.03) nm; IR (KBr) ν_{max} 3325, 2925, 2856, 1721, 1640, 1459, 1373, 1197, 1142 cm^{-1}; ^1H and ^{13}C NMR data, see Tables 1 and 2; HRESIMS *m/z* 438.3229 $[M + H]^+$ (calcd for $C_{26}H_{40}N_5O$, 438.3233).

Antibacterial assay

The *in vitro* antibacterial assay was carried out as reported before.[30] Vancomycin was used as positive control and displayed MIC_{90} values of 2, 1, 1, 1, and 0.5 μM against methicillin-susceptible *S. aureus* strain H608 and methicillin-resistant *S. aureus* strains 2010-260, 2010-210, 2010-292, and 2010-300, respectively.

Cytotoxicity assay

The effects of **1–7** on cell viability was determined using the Cell Counting Kit-8 (CCK-8). The human PC9, A549, HepG2, MCF-7, and U937 cell lines were obtained from the Institute of Biochemistry Cell Biology (Shanghai, China). Cells were seeded in 96 well plates (5×10^3 cells per well). After 24 h incubation, the cells were treated with various concentrations of **1–7** for 72 h. Then the CCK8 solution (10 μL) was added for additional 1 h incubation at 37 °C. The absorbance at 450 nm was measured in a microplate reader (spectra MAX190, Molecular Devices, USA). Independent experiments were performed in triplicate.

Acknowledgements

This research was supported by the National Natural Science Fund for Distinguished Young Scholars of China (81225023), the National Natural Science Fund of China (No. U1605221, 41428602, 41576130, 81502936, 41476121 and 81402844), and the Fund of the Science and Technology Commission of Shanghai Municipality (No. 14431901300 and 15431900900).

Notes and references

1 M. Mehbub, J. Lei, C. Franco and W. Zhang, *Mar. Drugs*, 2014, **12**, 4539–4577.
2 J. W. Blunt, B. R. Copp, R. A. Keyzers, M. H. G. Munro and M. R. Prinsep, *Nat. Prod. Rep.*, 2016, **33**, 382–431.
3 Y. Zhu, Y. Wang, B.-B. Gu, F. Yang, W.-H. Jiao, G.-H. Hu, H.-B. Yu, B.-N. Han, W. Zhang, Y. Shen and H.-W. Lin, *Tetrahedron*, 2016, **72**, 2964–2971.
4 T. Yasuda, A. Araki, T. Kubota, J. Ito, Y. Mikami, J. Fromont and J. i. Kobayashi, *J. Nat. Prod.*, 2009, **72**, 488–491.
5 D. B. Abdjul, H. Yamazaki, S.-i. Kanno, O. Takahashi, R. Kirikoshi, K. Ukai and M. Namikoshi, *J. Nat. Prod.*, 2015, **78**, 1428–1433.
6 J. J. La Clair and A. D. Rodríguez, *Bioorg. Med. Chem.*, 2011, **19**, 6645–6653.
7 Y. Tanaka and T. Katayama, *Nippon Suisan Gakkaishi*, 1982, **48**, 531–533.
8 J.-F. Hu, M. Kelly and M. T. Hamann, *Steroids*, 2002, **67**, 743–747.
9 D. Tasdemir, B. Topaloglu, R. Perozzo, R. Brun, R. O'Neill, N. M. Carballeira, X. Zhang, P. J. Tonge, A. Linden and P. Rüedi, *Bioorg. Med. Chem.*, 2007, **15**, 6834–6845.
10 H. Nakamura, H. Wu, J. i. Kobayashi, Y. Ohizumi, Y. Hirata, T. Higashijima and T. Miyazawa, *Tetrahedron Lett.*, 1983, **24**, 4105–4108.
11 H. Nakamura, H. Wu, J. Kobayashi, M. Kobayashi, Y. Ohizumi and Y. Hirata, *J. Org. Chem.*, 1985, **50**, 2494–2497.
12 F. Yang, M. T. Hamann, Y. Zou, M.-Y. Zhang, X.-B. Gong, J.-R. Xiao, W.-S. Chen and H.-W. Lin, *J. Nat. Prod.*, 2012, **75**, 774–778.
13 A. Medeiros Maria, A. Lourenço, R. Tavares Maria, M. Curto Maria João, S. Feio Sónia and C. Roseiro José, *Zeitschrift für Naturforschung C*, 2006, **61**, 472–476.
14 J. J. Morales and A. D. Rodríguez, *J. Nat. Prod.*, 1992, **55**, 389–394.
15 E. P. Stout, L. C. Yu and T. F. Molinski, *Eur. J. Org. Chem.*, 2012, **2012**, 5131–5135.
16 R. J. Capon and D. J. Faulkner, *J. Am. Chem. Soc.*, 1984, **106**, 1819–1822.
17 H. Nakamura, H. Wu, Y. Ohizumi and Y. Hirata, *Tetrahedron Lett.*, 1984, **25**, 2989–2992.
18 L. Calcul, K. Tenney, J. Ratnam, J. H. McKerrow and P. Crews, *Aust. J. Chem.*, 2010, **63**, 915–921.
19 T. Hattori, K. Adachi and Y. Shizuri, *J. Nat. Prod.*, 1997, **60**, 411–413.
20 H. Wu, H. Nakamura, J. i. Kobayashi, Y. Ohizumi and Y. Hirata, *Tetrahedron Lett.*, 1984, **25**, 3719–3722.
21 K. Ishida, M. Ishibashi, H. Shigemori, T. Sasaki and J. Kobayashi, *Chem. Pharm. Bull.*, 1992, **40**, 766–767.
22 X. Fu, F. J. Schmitz, R. S. Tanner and M. Kelly-Borges, *J. Nat. Prod.*, 1998, **61**, 548–550.
23 J. Appenzeller, G. Mihci, M.-T. Martin, J.-F. Gallard, J.-L. Menou, N. Boury-Esnault, J. Hooper, S. Petek,

S. Chevalley, A. Valentin, A. Zaparucha, A. Al-Mourabit and C. Debitus, *J. Nat. Prod.*, 2008, **71**, 1451–1454.

24 T. Kubota, T. Iwai, A. Takahashi-Nakaguchi, J. Fromont, T. Gonoi and J. i. Kobayashi, *Tetrahedron*, 2012, **68**, 9738–9744.

25 R. Fathi-Afshar and T. M. Allen, *Can. J. Chem.*, 1988, **66**, 45–50.

26 G. R. Pettit, Y. Tang, Q. Zhang, G. T. Bourne, C. A. Arm, J. E. Leet, J. C. Knight, R. K. Pettit, J.-C. Chapuis, D. L. Doubek, F. J. Ward, C. Weber and J. N. A. Hooper, *J. Nat. Prod.*, 2013, **76**, 420–424.

27 E. Piers and J. Y. Roberge, *Tetrahedron Lett.*, 1992, **33**, 6923–6926.

28 I. S. Marcos, N. García, M. J. Sexmero, P. Basabe, D. Díez and J. G. Urones, *Tetrahedron*, 2005, **61**, 11672–11678.

29 A. K. Bakkestuen and L.-L. Gundersen, *Tetrahedron*, 2003, **59**, 115–121.

30 W.-H. Jiao, J. Li, Q. Liu, T.-T. Xu, G.-H. Shi, H.-B. Yu, F. Yang, B.-N. Han, M. Li and H.-W. Lin, *Molecules*, 2014, **19**, 18025–18032.